Boletim da Sociedade Astronômica Brasileira, **35**, no. 1, 156-157

Simulated observations of intermediate redshift galaxies with the MOSAIC spectrograph for the Extremely Large Telescope

L. Béchade[1] & T. S. Gonçalves[1]

[1] Valongo Observatory, Federal University of Rio de Janeiro e-mail: lucab21@ov.ufrj.br, tsg@ov.ufrj.br

Abstract. This work aims to determine the limitations in terms of stellar mass and signal-to-noise ratio (S/N) to which MOSAIC, the multi-object spectrograph for the ELT, will be able to recover the star formation histories of galaxies at high redshift. We use the Bagpipes library to create synthetic spectra with multiple S/N, which are used to measure the spectral indices that allow us to constrain their star formation histories. We can therefore estimate an operational limit for MOSAIC by analyzing the incertitude of these spectral indices. We expect to use the synthetic spectra in the MOSAIC ETC soon in order to constrain the MOSAIC performance more accurately.

Resumo. Este trabalho visa determinar, em termos de massas solares e razão sinal-ruído (S/N), os limites para que o MOSAIC, espectrógrafo multi-objeto do ELT, seja capaz de recuperar o histórico de formação estelar de galáxias em alto *redshift*. Nós usamos a biblioteca Bagpipes para criar espectros sintéticos com múltiplos S/N, os quais são usados para medir os índices espectrais que permitem traçar seus históricos de formação estelar. Podemos, portanto, estimar um limite operacional para o MOSAIC através da anlálise das incertezas desses índices espectrais. Nós esperamos usar os espectros sintéticos na ETC do MOSAIC em breve para restringir a performance do MOSAIC mais precisamente.

Keywords. Galaxies: star formation – Instrumentation: spectrographs – Galaxies: evolution

1. Introduction

With the advent of the next generation of ground-based extremely large telescopes, such as the Extremely Large Telescope (ELT), the Thirty Meter Telescope (TMT) and the Giant Magellan Telescope (GMT), new opportunities for deep spectroscopic studies of distant, faint galaxies arise. To fulfill the requirements of a multi-object spectrogrph (MOS) for the ELT, the concept of MOSAIC was introduced (Evans et al. 2014). This work aims to determine the limitations in terms of signal-to-noise ratio (S/N) and stellar masses to which MOSAIC will be able to recover the star formation history (SFH) of galaxies at redshift $z \sim 2$.

2. The MOSAIC instrument

MOSAIC consists of two spectrographs: one for the near-infrared (NIR) wavelength range, and the other for the the optical wavelengths. MOSAIC will be a multi-object spectrograph with a wide field of view and three observational modes:

* High multiplex modes: Integrated-light (or coarsely resolved, via GLAO) observations of >100 objects.
  - High multiplex within the optical wavelength range.
  - High multiplex within the NIR.
* High-definition mode: Observations of tens of IFU channels at fine spatial resolution, with multi-object adaptive optics providing high-performance AO for selected sub-fields.
  - Multi-IFU within the NIR.

3. Methodology

We follow the method introduced by Kauffmann et al. (2002) to constrain SFH based on two stellar absorption line indices: the 4000 Å break strength and the Balmer absorption line index Hδ_A. We adopt the narrow definition of the 4000 Å break, introduced by Balogh et al. (1999) as the ratio of the average flux density in the bands 3850–3950 and 4000–4100 Å, denoted as $D_n(4000)$, which is given by

$$D_n(4000) = \frac{\sum_{\lambda=4000}^{\lambda=4100} F_\lambda}{\sum_{\lambda=3859}^{\lambda=3950} F_\lambda}, \quad (1)$$

where F_λ corresponds to the flux within λ wavelength. The $D_n(4000)$ index is correlated to the age of the galaxy. The opacity in the bluer region of the optical spectrum, due to the presence of ionized metals in old galaxies, leads to an accumulation of a large number of spectral lines in a narrow wavelength region, thus leading to a large ratio between the flux following the 4000 Å bandpass and the flux prior to it.

We define the Hδ_A using a central bandpass bracketed by two pseudo-continuum bandpasses (Worthey & Ottaviani 1997):

$$H\delta_A = \sum_{\lambda=4083.5}^{\lambda=4122.25} \left(1 - \frac{F_\lambda}{F_{\lambda,\,cont}}\right), \quad (2)$$

where F_λ corresponds to the flux within λ wavelength (Hδ bandpass) and $F_{\lambda,\,cont}$ is the continuum flux. The peak of Hδ absorption line strength arises in galaxies that experienced a burst of star formation that ended $\sim$ 1 Gyr ago. The death of O stars leaves a spectral energy distribution dominated by A, F, and late B type stars, which have strong intrinsic Balmer absorption features.

We use data from the X-shooter Spectral Library (Verro et al. 2022b), as well as the Bagpipes Python library (Carnall et al. 2018) to create synthetic spectra of τ model exponentially declining SFH galaxies, with $\tau \sim 1$ Gyr. We artificially introduce white noise at different levels, ranging from 0.1 to 20 per pixel. We then compare them with a reference ideal spectrum

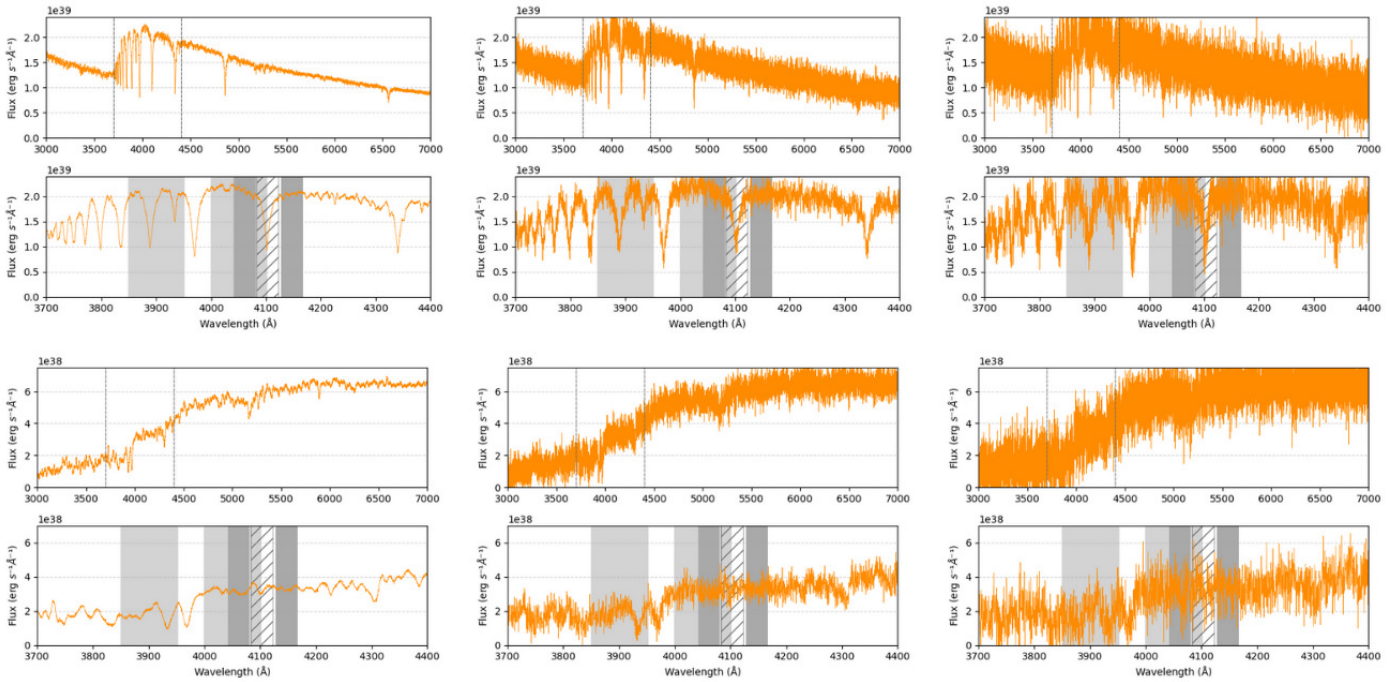

Figure 1. Spectra of a 1 Gyr galaxy (top), with visible Balmer absorption features, and a 10 Gyr galaxy (bottom), with strong $D_n(4000)$ break, plotted for S/N 100, 10, and 5 (left to right). Each spectrum is plotted in the restframe over the intervals 3000-7000 Å (top subpanels) and 3700–4400 Å , for a detailed zoom of the region containing the absorption features used for SFH constraining (bottom subpanels). The light gray-shaded regions indicate the bandpasses over which the $D_n(4000)$ index is measured. The dark gray regions show the pseudocontinua for the $H\delta_A$ index, while the hatched region shows the $H\delta$ bandpass.

from the stellar population models. In order to understand the statistical variations over the spectral indices uncertainties, we produce 1000 noisy spectra at each S/N level. Fig. 1 shows examples of spectra created with Bagpipes for a 1 Gyr and a 10 Gyr galaxy, with the $D_n(4000)$ and $H\delta_A$ indices highlighted, for 3 different S/N.

4. Results and perspectives

For each galaxy, we constrain the S/N required to accurately measure the $D_n(4000)$ and $H\delta_A$. We assume, provisionally, an upper limit to the standard deviation and absolute systematic error of 1 for the $D_n(4000)$, and 0.2 for $H\delta_A$ as an estimate for a reliable S/N constraint.

We determine that a minimum S/N of 2.8 is necessary to achieve the required uncertainty thresholds for a 1 Gyr-old galaxy, while that value is 6.9 for the older galaxy. Evans et al. (2015) simulated Ly-α emitters multiplex observations with MOSAIC at $z \sim 2$, estimating to reach $S/N = 10$ in 10 h, for a point-source of $J_{AB} = 26$ mag. We therefore expect the ELT to achieve, with MOSAIC, the S/N of 2.8 in < 1 h and 6.9 in < 5 h of integration time for galaxies with mass at the order of $10^9\ M_\odot$, with $K_{AB} \sim -19$ mag, at $z \sim 2$. Fig. 2 shows the S/N limits obtained from the statistical fluctuations for each one of the 1000 measures of $D_n(4000)$ and $H\delta_A$, for each one of the 200 S/N.

We expect to set a proper S/N threshold soon by analyzing the impact of the individual standard deviation and systematic errors over the $D_n(4000)$ and $H\delta_A$ measures for at least 100 ages, within the 0.1 to 10 Gyr span. Another key part in our future work is to calculate the star formation acceleration (SFA) from the SFH, following the method introduced by Martin et al. (2017). We then expect to use our synthetic spectra in the MOSAIC ETC (under development), allowing us to estimate with more accuracy the MOSAIC performance and limitations.

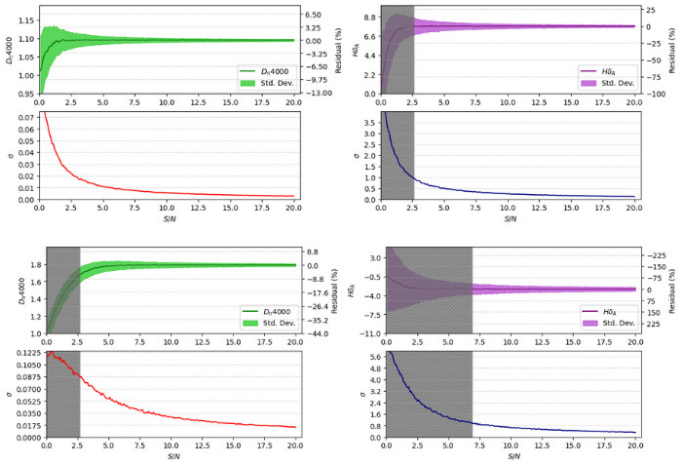

Figure 2. Median $D_n(4000)$ and $H\delta_A$, as well as their respective standard deviation, for a 1 Gyr galaxy (top) and a 10 Gyr galaxy (bottom). The gray-hatched region represents the region within which the S/N is preliminarily determined as insufficient in order to reliably recover the original index values.

References

Balogh, M. et al. 1999, *The Astrophysical Journal*, 527, 54;
Carnall, A. C. et al. 2018, *Monthly Notices of the Royal Astronomical Society*, 480, 4379;
Evans, C. J. et al. 2014, *Proceedings of the SPIE*, 9147;
Evans, C. J. et al. 2015, *arXiv astro-ph*, 1501;
Kauffmann, G. et al. 2002, *Monthly Notices of the Royal Astronomical Society*, 341, 33;
Martin, D. C. et al. 2017, *The Astrophysical Journal*, 842, 20;
Verro, K. et al. 2022, *Astronomy & Astrophysics*, 661, A50;
Worthey, G., Ottaviani, D. L., 1997, *The Astrophysical Journal Supplement Series*, 111, 377.